Applied Clay Science 230 (2022) 106703

Contents lists available at ScienceDirect

Applied Clay Science

journal homepage: www.elsevier.com/locate/clay

Technical Note

Antimicrobial ceramic foam composite air filter prepared from Moroccan red clay, phosphate sludge waste and biopolymer

László Mérai [a], Ágota Deák [a], Mohamed A. Harech [b], Mohamed M. Abdelghafour [a,c], Dániel Sebők [d], Áron Ágoston [a], Szabolcs P. Tallósy [e], Tamás Szabó [a], Younes Abouliatim [f], Mohamed Mesnaoui [b], Lahbib Nibou [g], Ákos Kukovecz [d], László Janovák [a,*]

[a] Department of Physical Chemistry and Materials Science, University of Szeged, H-6720 Szeged, Hungary
[b] Laboratory Sciences Inorganic Materials and their Applications: Condensed and environmental chemistry team, FSSM, Cadi Ayyad University, Morocco
[c] Department of Chemistry, Faculty of Science, Zagazig University, Zagazig 44519, Egypt
[d] Department of Applied and Environmental Chemistry, University of Szeged, H-6720 Szeged, Hungary
[e] Institute of Surgical Research, Albert Szent-Györgyi Medical School, University of Szeged, Hungary
[f] Engineering and Processes and Environment Laboratory, Higher School of Technology, Hassan II University, Casablanca, Morocco
[g] Systems Engineering and Applications Laboratory, ENSAM, Cadi Ayyad University, Morocco

ARTICLE INFO

Keywords:
Safi clay
Chitosan
Polyvinyl alcohol
Antimicrobial
Escherichia coli
Airborne microorganism

ABSTRACT

The COVID-19 pandemic has highlighted the importance of air sterilization and disinfection. Besides the regular cleaning and disinfection of surfaces it is at least as important to reduce the number of airborne microorganisms as they are known to play an important role in the spreading of different infections.

Herein, we report a facile preparation of a porous air filter ceramic composite material, suitable for the effectively eliminating airborne microorganisms. The antimicrobial activity of the ceramic foam could be attributed to a thin chitosan biopolymer layer immobilized on the ceramic surface. Furthermore, as the ceramic foam was prepared on phosphate sludge waste and Moroccan red clay basis, this research opens new routes towards the valorization of solid industrial or mining wastes or other yet unused abundant materials, as well.

1. Introduction

The ongoing worldwide epidemic crisis and the emerging antibiotic resistance of pathogens urge the development of new disinfection technologies (Boldogkői et al., 2021; Abdelghafour et al., 2022). Besides finding the proper medications, the spotlight of related scientific research is shed on developing novel preventive measures meant to hinder the spreading of infections. Aside from the application of non-preferred potent biocides, such as sodium hypochlorite, most of these technologies use other reactive chemical species (e.g., ozone) (Borges et al., 2017), radiations (e.g., UV) (Tawema et al., 2016; de Oliveira et al., 2021), UV- light activated photocatalysts (such as TiO_2) (Abdelghafour et al., 2020; Boldogkői et al., 2021; Abdelghafour et al., 2022), noble metal nanoparticles (Noralian et al., 2021), metal salts (Parvinzadeh Gashti and Dehghan, 2020) and high-performance filters (HEPA) (Kim et al., 2021) to eliminate air- and waterborne pathogens before they can come in contact with the human body.

Another preferred way can be the application of antibacterial polymers (Kamaruzzaman et al., 2019; Qiu et al., 2020). The antibacterial activity of polymers such as chitosan can be attributed to positively charged functional groups or sidechains (e.g., protonated amino groups), which contributes to the unfolding of bacterial membranes (Chung and Chen, 2008; Kamaruzzaman et al., 2019; Qiu et al., 2020).

Besides preserving human health, the preservation of the environment is also of the highest priority; therefore, the efforts towards the valorization of abundant inorganic industrial waste materials show a globally emerging trend (Goodman, 2020; Hossain and Roy, 2020; Gautam et al., 2021; Wen et al., 2021). Potential examples of such materials are the phosphate sludge (PS) or the Moroccan red clay, which were previously utilized, e.g. as ingredients in ceramic membrane production for wastewater purification (Mouiya et al., 2017; Mouiya et al., 2018). To expand the application scope of porous phosphate sludge-clay (PS-clay) ceramic structures, preparation of ceramic foams would also be beneficial. The preferred routes of ceramic foam production are the different templating methods (Peng et al., 2000; Stipniece et al., 2020; Liu et al., 2021), that utilize sacrificial foam templates (e.g., sponges) or

* Corresponding author.
E-mail address: janovakl@chem.u-szeged.hu (L. Janovák).

https://doi.org/10.1016/j.clay.2022.106703
Received 25 May 2022; Received in revised form 15 August 2022; Accepted 13 September 2022
Available online 23 September 2022

porogenes (e.g., combustible organic materials, inorganic carbonates), which form pores during the firing process. The templating techniques offer good reproducibility and control over morphology with the slightest chance of foam collapse, which makes them more attractive than direct foaming scenarios, in which a foaming gas is bubbled through the ceramic suspension before drying and firing (Barg et al., 2008; Ahmad et al., 2013; Li et al., 2014).

To address the need for the valorization of two abundant inorganic materials and to achieve new options in air cleaning, we prepared ceramic foams on phosphate sludge and red clay basis in this work. To achieve structural integrity and homogeneity, an in-situ templating method was applied, exploiting the foam-forming capability of polyvinyl alcohol (PVA) in the presence of sodium borohydride ($NaBH_4$) (Nunes et al., 2016; Hall, 2019). The antimicrobial properties were elaborated upon coating the ceramic foams with chitosan biopolymer.

2. Materials and methods

2.1. Preparation of the PS-clay foams

The used phosphate sludge-clay (PS-clay) powder mixture - which was kindly provided by the Condensed and environmental chemistry team (FSSM, UCA, Morocco) - contained 50 wt% Moroccan phosphate sludge and 50 wt% red Safi-clay. The major chemical composition of red clay given in weight percentages is the following: SiO_2 (52.79%), Al_2O_3 (17. 44%), Fe_2O_3 (5.85%) (Harech et al., 2021). The phosphate sludge is rich in P_2O_5 (16.83%) and CaO (31.44%). It also contains SiO_2 (27.48%), low quantities of Al_2O_3 (2.41%) and Fe_2O_3 (0.93%) (Harech et al., 2021).

Polyvinyl alcohol (PVA) foam templates were prepared by adding $NaBH_4$ (a.r., Reanal, Hungary) to 100 g/L aqueous PVA solutions (M_w = ~ 47 kDa, degree of hydrolysis: 86–89%, Nagart Ltd., Hungary) with 18 mg $NaBH_4$ to 3 mL PVA solution ratio. The $NaBH_4$ was dispersed by vigorous stirring and the solutions were left for 1 h at room temperature to let the foaming of the formed crosslinked, gelous substance take place. To form PS-clay foams, 1.8 g of PS-clay powder mixture was added to each 3 mL of 100 g/L of PVA solution and thoroughly dispersed before the addition of the $NaBH_4$ (18 mg $NaBH_4$ / 3 mL PVA solution).

The PS-clay/PVA foams were fired in an oven according to the following heating protocol: 250 °C (4 h; drying) ➔ 450 °C (1 h; annealing, decomposition of organic materials) ➔ 750 °C (1 h; dehydroxylation and calcination) ➔ 1100 °C (2 h; recrystallization annealing) applying 5 °C/ min heating rate (Mouiya et al., 2018).

To form an electrostatically adhered antimicrobial polymer layer on the fired ceramics, the foams were dipped (100 g solids in 1 L dispersion) in 10 g/L Chitosan Medium (Chitosan-M; deacetylation degree: 75–85%; Sigma Aldrich) solution (containing 1 vol% acetic acid) for 24 h. The coated foams were then dried at 40 °C for 24 h.

2.2. Methods of sample characterization

The X-ray computed tomography (CT) analysis of the PVA foam, the initial PS-clay foam, and the Chitosan-M-coated PS-clay foam was performed with a Multiscale X-ray nanotomograph (Skyscan 2211, Bruker), equipped with a CCD camera. The applied acceleration voltage was 80 kV, while the pixel resolution was 2 μm.

The X-ray diffractograms of the initial and fired PS-clay mixture and of the pulverized PS-clay foam were recorded using a Philips X-ray-diffractometer (XRD) with CuKα ($\lambda = 0.1542$ nm) as the radiation source at ambient temperature in the 2–70° (2Θ) range applying 0.02° (2Θ) step size.

The surface morphology of the PVA foam, the PS-clay foam after firing and the PS-clay foam after adsorption of Chitosan-M were examined with a SEM – Hitachi S-4700 field emission scanning electron microscope (secondary electron detector, acceleration voltage: 15 kV). The elemental distribution was studied using a Röntec EDS detector.

Surface charge values of the ceramic foam and Chitosan-M were measured by

particle charge detector (PCD-04 Particle Charge Detector; Mütek Analytic GmbH, Germany)

with manual titration. During the titration process the surface charge of ceramic particles in 10 mL c = 0.1 g/L aqueous suspension was compensated with 0.1 g/L cationic Chitosan-M solution (containing 0.125 vol% acetic acid, pH = 4.26) and 0.01 g/L hexadecyl pyridinium chloride (HDPCl) solutions at 7.64 initial pH. The equimolar amounts of surfactant and polymer were calculated and specified to the amount of 1 g examined specimen (eq/g).

Thermogravimetric (TG) analysis (Mettler-Toledo TGA/SDTA 851e Instrument) was used to study the heat degradation of the initial PS-clay foam and the PS-clay foam after adsorption of cationic polymers. The heating rate of the sample was 5 °C/min from 25 to 500 °C in synthetic air atmosphere.

During the liquid-phase TOC (Total Organic Carbon) adsorption experiments, 0.2 g ceramic foam was dispersed (100 g/L) in 2 mL acidic chitosan solutions (acetic acid) with varying concentrations (g/L; with the corresponding acetic acid contents in brackets): 0.625 (0.78), 1.25 (1.56), 2.5 (3.13), 5 (6.25) and 10 (12.50). After 24 h adsorption time at room temperature (homogenization via continuous shaking), the liquid phase of the mixtures was sampled, and the adsorbed amounts of organics was determined applying the TOC method (Analytik Jena multi N/C 2100S TOC instrument).

The solid-phase Total Carbon (TC) determination experiments were performed by the same instrument, equipped with a horizontal double furnace solids module. The measurements were run at 900 °C, applying 10 min integration time and 36 mg portions of the coated ceramic foam.

The FT-IR spectra of the initial PS-clay powder mixture, Chitosan-M powder and the pulverized ceramic foams were recorded applying a Jasco FT-IR 4700 instrument (Jasco Inc., Maryland, United States) in attenuated total reflection (ATR) mode. The measurement parameters were the followings: 2 cm^{-1} optical resolution, 2 mm/s scanning speed, 500–4000 cm^{-1} wavenumber range.

2.3. Antimicrobial studies

The antimicrobial experiments were based on our previous publications (Deák et al., 2015; Tallósy et al., 2016). In our antibacterial tests on Chitosan-M solutions, *Escherichia coli* ATCC 29522 was used as test microorganism. During the experiments 0.1 mL portions of bacterial suspension with a concentration of 9.7×10^8 CFU/mL (CFU: Colony Forming Units) were used to inoculate Mueller-Hinton media in a Petri dish. Under the applied experimental conditions, the initial surface bacterial concentration was 1.79×10^6 CFU/cm^2. Then, a dilution series were prepared from the initial aqueous Chitosan-M solution in the concentration range of 0–10 g/L. Ten microliters from each sample were pipetted onto the surface of the bacterial biofilm. Finally, the media were incubated at 37 °C overnight, and the minimum inhibitory concentration (*MIC*) value of Chitosan-M was determined from the size of the emerging inhibition zones (cm).

The antimicrobial air-filtering effectivity of Chitosan-M-coated ceramic foams was studied at indoor conditions (in an office with dimensions of 5.5 m × 3.5 m × 3.8 m), applying two 8 cm × 5 cm × 2 cm foam pieces as filters, placed atop the sampling hole of an RCS PLUS air sampler (Bio-Test Ltd., Budapest, Hungary). Parallel experiments were also run without the Chitosan-M-coated ceramic foam filter.

The air sampler was adjusted to collect 1000 L of air transmitting to the agar strips (Merck, Budapest, Hungary) on which the microorganisms (airborne bacteria and fungi) can adhere and form visible colonies after an incubation time of 16 h at 37 °C.

The colony forming units (CFU/m^3) were counted on nutrient agar strips and compared to the null-point sample (initial point of the experiment). Three parallel experiments were carried out in each case, and the counts of different adhering microorganisms (CFU/m^3) were

averaged.

3. Results and discussion

3.1. Preparation and physicochemical characterization of ceramic foams

The templates of the ceramics were prepared through the direct crosslinking and foaming of PVA by $NaBH_4$, as it is shown in Fig. 1. Upon the addition of $NaBH_4$ to aqueous PVA solutions, borate ions form (crosslinking), and H_2 gas evolves (foaming) (Nunes et al., 2016), while PVA does not undergo any chemical transformation. If PS-clay powder mixture is dispersed in the initial PVA solution, the foam itself acts as a fireable template to the final ceramic product. The resulting PS-clay powder-containing borate-crosslinked PVA foams were fired at 1100 °C according to an already published method, previously applied on similar ceramics [15].

As the SEM- and CT-imagery in Fig. 2 show, the PVA foams have an open pore structure with heterogenous pore size distribution, falling within the 0.1–1 mm diameter-range (porosity: 93.9%). In comparison, the fired ceramic foams preserve a similar open structure and pore size range (porosity: 93.9%), which proves the excellent templating capability of the crosslinked PVA foam. Furthermore, upon the XRD analysis of the pulverized PS-clay foams, the characteristic major crystalline phases of PS-clay ceramics (Mouiya et al., 2017; Mouiya et al., 2018) were found in the sample (the diffractograms and their further explanations can be found among the Supplementary Materials; Fig. S1), such as quartz (JCPDS: 46–1045), hematite (JCPDS: 86–055) and fluorapatite (JCPDS: 01–076-0558).

The ceramic foams (like most oxide and phosphate ceramics (Mullet, 1997; Nakamura et al., 2002; Árki et al., 2019)) possess a negative net surface charge (or point of zero charge around pH = 7), as it was proven by surface charge titration measurements (Fig. 3.). This means that positively charged molecules or particles can be electrostatically adsorbed on their surfaces. An ideal candidate for such experiments is the antibacterial chitosan (Chung and Chen, 2008; Kamaruzzaman et al., 2019; Qiu et al., 2020), which possesses net positive charge in acidic media due to the protonation of its amino groups ($-NH_2$) (Reis et al., 2021; Sirviö et al., 2021). As Fig. 3. shows, it was shown that during surface charge titrations, that the positively charged chitosan can neutralize the negative charge ($-8{,}5 \times 10^{-6}$ eq/g measured with cationic HDPCl at pH = 7.66) excess of ceramic foam surfaces (charge neutrality at 1.47 mg/g; $m_{adsorbed\ Chit\text{-}M}/m_{ceramic\ foam}$), which indicates electrostatic interactions between the oppositely charged ceramic foam and the antibacterial macromolecules. As the result of this, electrostatic chitosan adsorption is preferred on the ceramic surface: the adsorbed amounts are displayed in Fig. S2. As it can be seen, until around $c_e = 5$ g/L equilibrium chitosan concentration, ~1.5 mg/g chitosan was adsorbed on the surface of ceramic foam which is in good agreement with the surface charge titration results (1.47 mg/g, Fig. 3.). However, further increasing the chitosan concentration ($c_e > 5$ g/L) a significant increase can be observed on the adsorbed amount of chitosan. This multi-stage adsorption of polymers in porous media and its concentration dependence is well- known from the literature (Al-Hajri et al., 2018) which is plausibly due to the entanglement of the macromolecules through their tails and loops (Zhang and Seright, 2013).

The adsorbed amount of chitosan on ceramic foam was also determined via TG and solid- phase TC and TOC measurements, as well (Fig. S3): in the case of the adsorption from a 10 g/L (1%) Chitosan-M solution, the resulting coated ceramic product contained 0.9 wt% adsorbed polymer (9.4 mg polymer/g ceramic foam). During the examination of the dry, coated (adsorption from 10 g/L or 1% Chitosan-M solution) ceramic foam (solid-phase TC), the polymer content was calculated to be 0.30–0.36 wt% (3.0–3.7 mg polymer/g ceramic foam), based on the given 75–85% deacetylation degree of the product.

Besides examining the solid product, the chitosan adsorption was studied via liquid-phase TOC-measurements, as well: according to this approach, the adsorbed amount of the polymer fell within the 0.5–5.0 mg/g range (The determined adsorption isotherm can be found in the supplementary material Fig. S2), which is in good accordance with the solid-phase TC- or TG results, and with the results of particle charge titrations, as well. (Fig. 3.)

The chitosan coverage of the surfaces was studied via EDX-spectroscopy (The EDX-spectra can be seen in Fig. S4). As Fig. 4. shows, according to the spectral analysis, the initial ceramic foam only consists of inorganic elements (oxygen, silicon, aluminium, and calcium in higher amounts), while the surface of the Chitosan-M-coated ceramic foam contains 15.36 at.% carbon, indicating a relatively high and homogenous surface coverage by the organic material. As the EDX measurements gave a slightly different result, one must consider that EDX provides spectral information exclusively from the surface layer (upper 1–2 μm), while the other determination techniques take the whole amount of the adsorbent into account.

Despite they bear no quantitative information, the recorded FT-IR spectra (Fig. S5) also showed the presence of Chitosan-M on the ceramic foam surfaces, which was indicated by the high relative intensity of the C—O stretching band with the maximum adsorption at 1024 cm^{-1} (Socrates, 2001).

3.2. Antibacterial effect of ceramic foams on indoor air

Although the antimicrobial activity of chitosan is well known from the literature (Fei Liu et al., 2001; Chung and Chen, 2008;

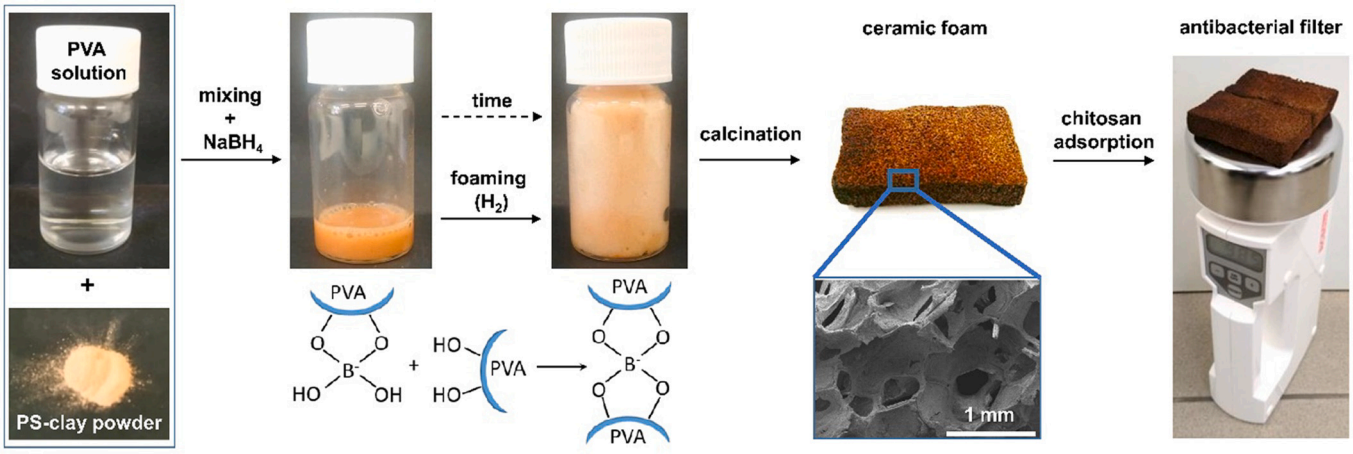

Fig. 1. Preparation and application scheme of Chitosan-M-coated, PVA-templated antimicrobial ceramic foams.

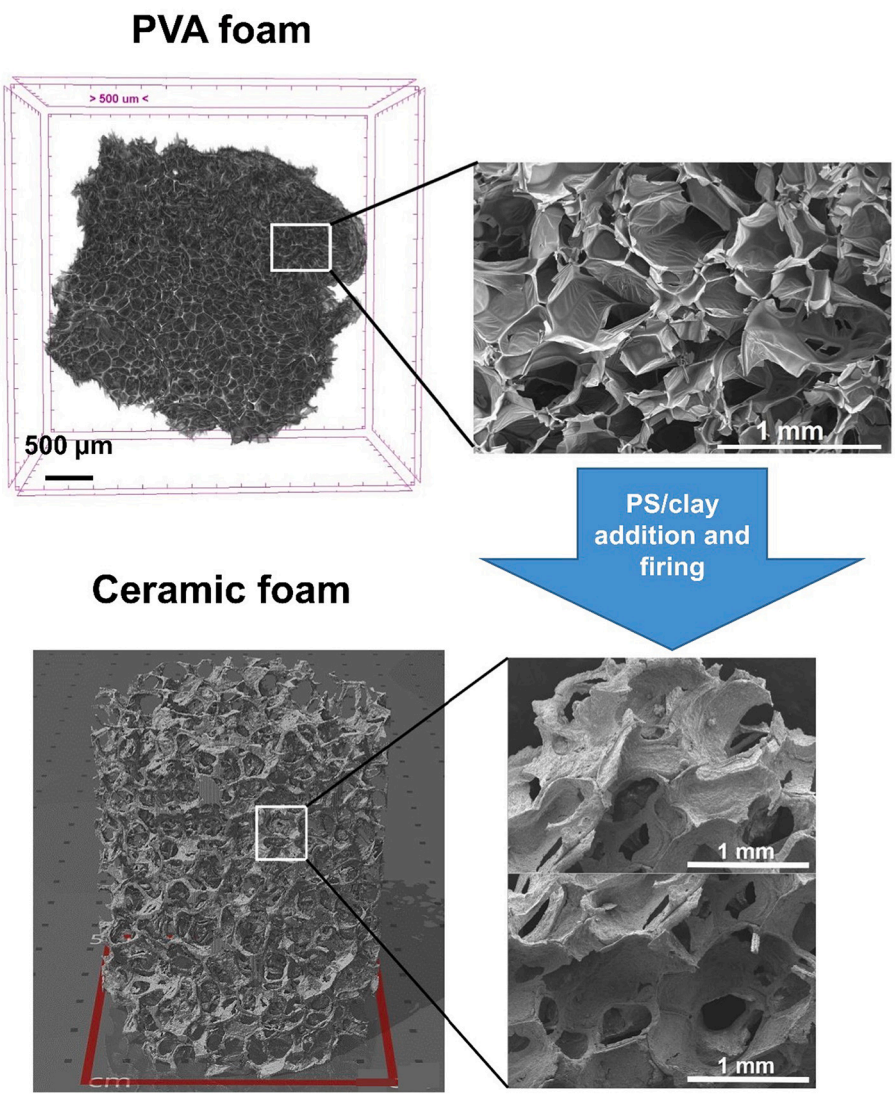

Fig. 2. Structure of PVA-foam and fired PS-clay ceramic foam in SEM (right) and CT (left) images.

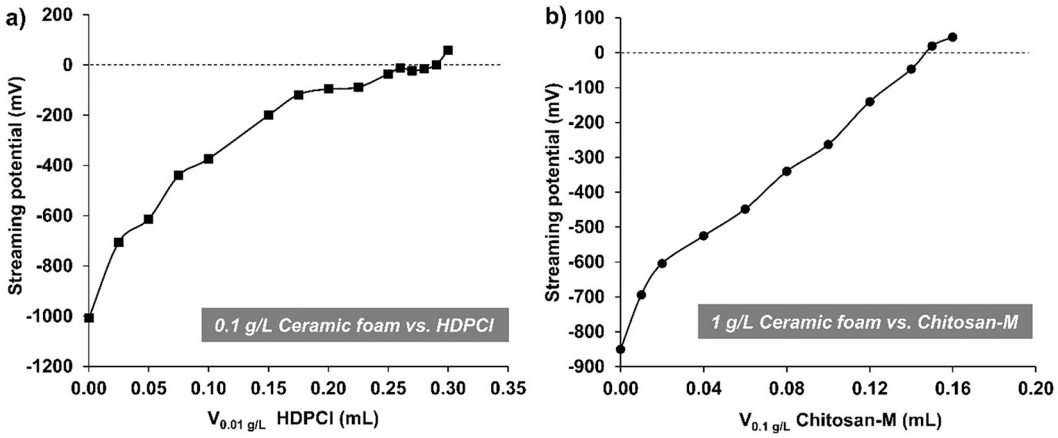

Fig. 3. Surface charge titration curves of fired PS-clay ceramic foam titrated with cationic HDPCl surfactant solution a) and negatively charged PS-clay ceramic foam titrated with Chitosan-M polycation solution b).

Kamaruzzaman et al., 2019; Qiu et al., 2020), the reported efficiencies can vary with the experimental conditions (bacterial strain, inoculation medium etc.). According to our test results, the antimicrobial activity of Chitosan-M solutions was considerable only above 10 and 5 g/L (0.5–1 mixed%) (1 mixed% = 1 g solute/0.1 L solution) of chitosan concentration (Fig. 5 a), at which zones of inhibition could be observed (d =

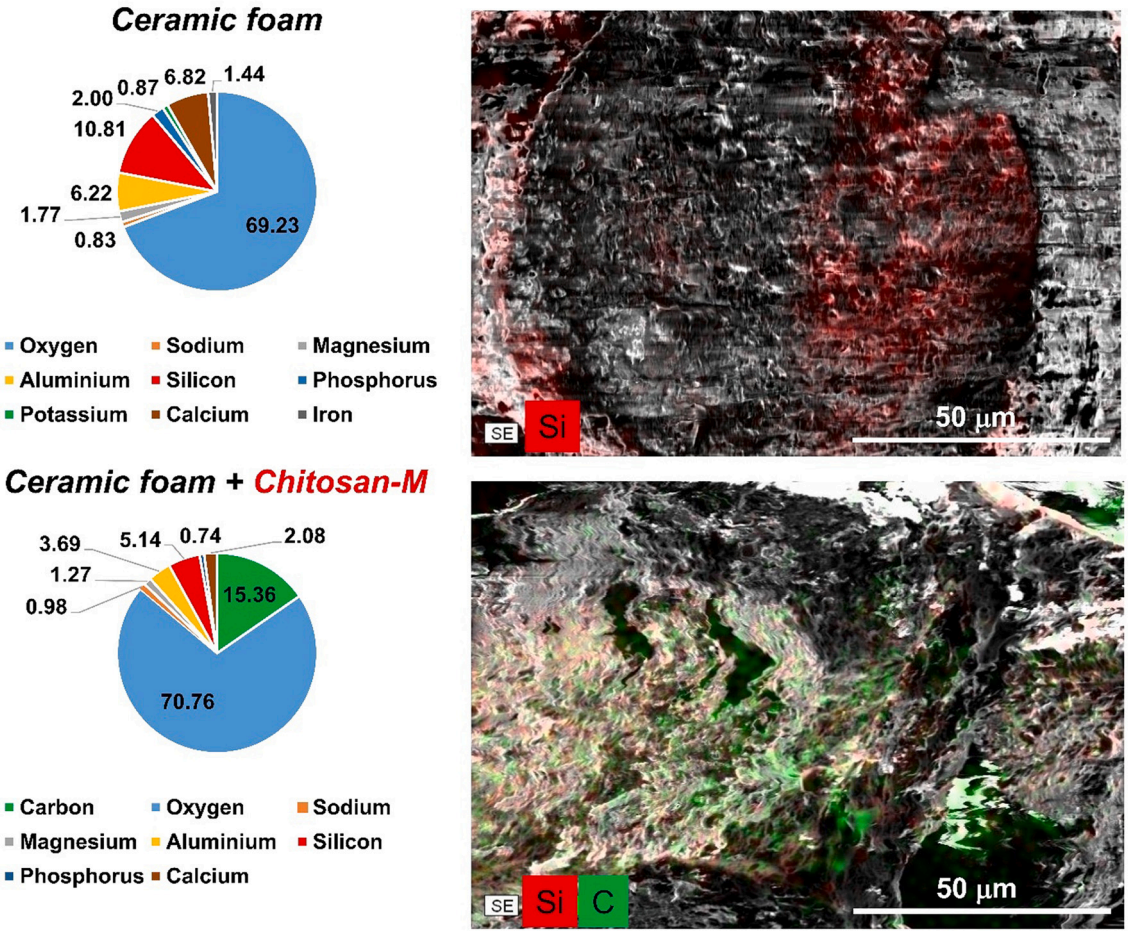

Fig. 4. EDX-SEM elemental mapping (for C and Si) and the corresponding elemental composition (magnification: 1000×) of Chitosan-M-coated and initial PS-clay ceramic foam surfaces.

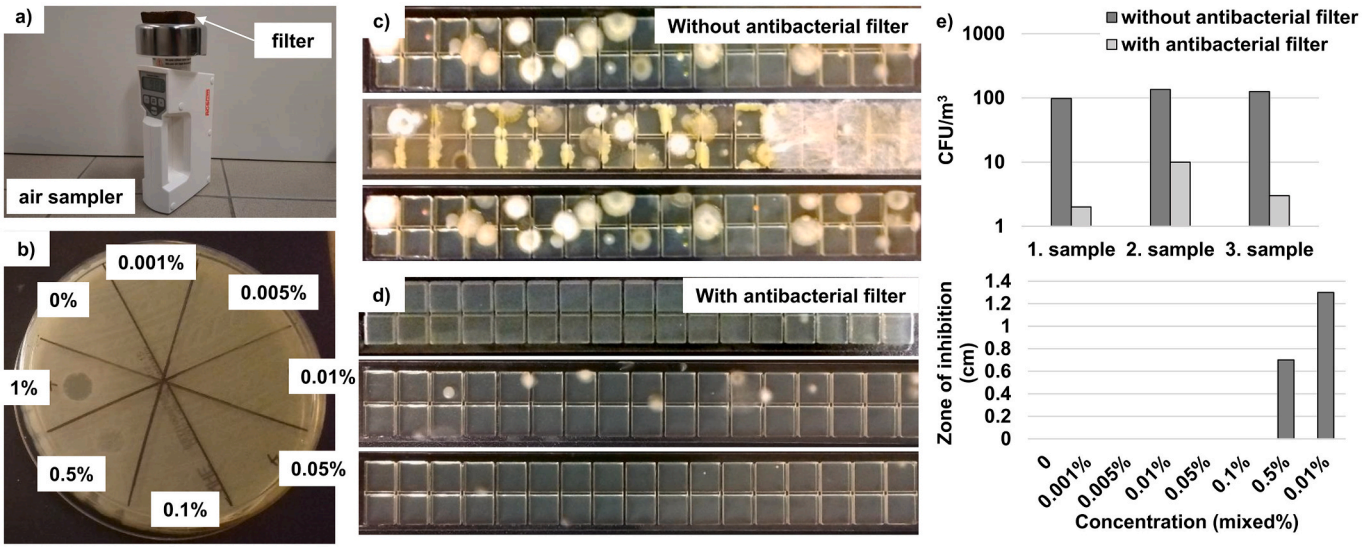

Fig. 5. Experimental setup of antimicrobial measurements against airborne microorganisms a) inhibition zones of Chitosan-M solution (10 µL) with different concentrations (0–10 g/L, or 0–1 mixed%) on *Escherichia coli* ATCC29522 b), bacterial and fungal colonies from filtered and unfiltered air c), evaluation of the antimicrobial effect of the Chitosan-M-coated PS-clay foam in air d), and antibacterial susceptibility testing on surface as a function of concentration of the Chitosan-M solution e).

~0.5 mm). As Fig. 5 b) shows, the Chitosan-M-coated ceramic foams (coated in 10 g/L Chitosan-M) could reduce the number of colony forming units during air filtration experiments (illustrated in Fig. 5 c) from 119 ± 19 CFU/m^3 to 5 ± 4 CFU/m^3 indicating the desired antimicrobial character. The obtained CFU values are comparable to those of similar air-filtration experimental setups in the literature, as well (Napoli et al., 2012).

Despite numerous examples of antimicrobial ceramic filtration bodies are present in the literature, most of the attention is paid to water cleaning (Chaukura et al., 2020; Ferreira et al., 2021), while the air disinfection (Dutheil de la Rochère et al., 2019; Wang et al., 2021) and the utilization of waste- and abundant clay materials in such systems are somewhat marginalized subjects. Therefore, the presented ceramic composite offers a novel, greener approach towards air-cleaning.

4. Conclusion

Herein we reported the preparation and characterization of efficient antimicrobial filter material, made of Moroccan red clay, phosphate sludge, and biopolymers (PVA, Chitosan Medium).

The ceramic foams were obtained through in-situ templating via the foaming of PVA in the presence of $NaBH_4$ and the subsequent high-temperature (1100 °C) firing. The porous (93.90% porosity) foam structures were examined by SEM and X-ray micro-CT techniques, while the composition was studied by XRD and EDX-spectroscopy.

According to the results of antimicrobial test, the room air, filtered with the ceramic foam samples, coated with ~10 mg/g (~1 mixed%) Chitosan-M only could produce significantly lower numbers of airborne bacteria and fungi (119 ± 19 CFU/m^3 to 5 ± 4 CFU/m^3) on the model inoculation medium. This highlights that we managed to fabricate an efficient air-cleaning porous ceramic-based nanocomposite material by using cheap and abundant inorganic raw materials and biopolymers in an easy and environmentally friendly process that successfully enables the valorization of phosphate sludge deposits. Besides achieving antimicrobial character, the present selection of starting materials is in line with the general burgeoning interest for the development of greener and more cost-efficient infection prevention technologies.

Although this paper only discusses the preparation and characterization of a specific type of coated foam, the scope of application and/or the antimicrobial efficacy could be fine-tuned by changing the porosity or the chitosan coverage by adjusting the preparation conditions e.g., crosslinker content in the templating PVA foam, different Chit-M concentrations during dip-coating and we suggest that these aspects should be thoroughly investigated.

CRediT authorship contribution statement

László Mérai: Investigation, Writing – original draft, Writing – review & editing, Visualization. **Ágota Deák:** Investigation, Visualization. **Mohamed A. Harech:** Writing – original draft. **Mohamed M. Abdelghafour:** Investigation. **Dániel Sebők:** Investigation, Visualization. **Áron Ágoston:** Investigation, Visualization. **Szabolcs P. Tallósy:** Investigation. **Tamás Szabó:** Conceptualization, Funding acquisition. **Younes Abouliatim:** Conceptualization, Funding acquisition, Resources, Supervision. **Mohamed Mesnaoui:** Writing – original draft. **Lahbib Nibou:** Resources. **Ákos Kukovecz:** Resources. **László Janovák:** Conceptualization, Writing – original draft, Writing – review & editing, Funding acquisition, Project administration, Resources, Supervision.

Declaration of Competing Interest

The authors declare that they have no known competing financial interests or personal relationships that could have appeared to influence the work reported in this paper.

Data availability

Data will be made available on request.

Acknowledgements

The authors are very thankful for the financial support from the Moroccan -Hungarian Joint Research project no. 2018-2.1.10-TÉT-MC-2018-00005 and from the National Research, Development and Innovation Office (GINOP-2020-1.1.2-PIACI-KFI-2021-00193 and GINOP-2019-1.1.1-PIACI-KFI-2019-00334). This paper was also supported by the ÚNKP-22-5 and UNKP-21-4-SZTE-510 New National Excellence Program of the Ministry for Innovation and Technology from the source of the National Research, Development and Innovation Fund and by the János Bolyai Research Scholarship of the Hungarian Academy of Sciences. The authors are also very thankful for the financial support from the Hungarian Scientific Research Fund (OTKA) K 132446. M.M.A. is funded by scholarship under the joint executive program between the Arab Republic of Egypt and Hungary. M.M.A. acknowledges Stipendium Hungaricum for his PhD scholarship.

Appendix A. Supplementary data

Supplementary data to this article can be found online at https://doi.org/10.1016/j.clay.2022.106703.

References

Abdelghafour, M.M., Deák, Á., Mérai, L., Ágoston, Á., Bélteki, R., Sebők, D., Dékány, I., Janovák, L., 2020. Photocatalytic elimination of interfacial water pollutants by floatable photoreactive composite nanoparticles. Environ. Pollut. 266, 115285 https://doi.org/10.1016/j.envpol.2020.115285.

Abdelghafour, M.M., Imre-Deák, Á., Mérai, L., Janovák, L., 2022. Photoreactive Composite Coatings with Tunable Surface Wetting Properties and their Application Possibilities, pp. 209–256. https://doi.org/10.1007/978-3-030-77371-7_8.

Ahmad, S., Latif, M.A., Taib, H., Ismail, A.F., 2013. Short Review: Ceramic Foam Fabrication Techniques for Wastewater Treatment Application. Adv. Mater. Res. 795, 5–8. https://doi.org/10.4028/www.scientific.net/AMR.795.5.

Al-Hajri, S., Mahmood, S., Abdulelah, H., Akbari, S., 2018. An Overview on Polymer Retention in Porous Media. Energies 11, 2751. https://doi.org/10.3390/en11102751.

Árki, P., Hecker, C., Tomandl, G., Joseph, Y., 2019. Streaming potential properties of ceramic nanofiltration membranes – Importance of surface charge on the ion rejection. Sep. Purif. Technol. 212, 660–669. https://doi.org/10.1016/j.seppur.2018.11.054.

Barg, S., Soltmann, C., Andrade, M., Koch, D., Grathwohl, G., 2008. Cellular Ceramics by Direct Foaming of Emulsified Ceramic Powder Suspensions. J. Am. Ceram. Soc. 91, 2823–2829. https://doi.org/10.1111/j.1551-2916.2008.02553.x.

Boldogkői, Z., Csabai, Z., Tombácz, D., Janovák, L., Balassa, L., Deák, Á., Tóth, P.S., Janáky, C., Duda, E., Dékány, I., 2021. Visible Light-Generated Antiviral effect on Plasmonic Ag-TiO2-based Reactive Nanocomposite Thin Film. Front. Bioeng. Biotechnol. 9 https://doi.org/10.3389/fbioe.2021.709462.

Borges, G.Á., Elias, S.T., da Silva, S.M.M., Magalhães, P.O., Macedo, S.B., Ribeiro, A.P.D., Guerra, E.N.S., 2017. In vitro evaluation of wound healing and antimicrobial potential of ozone therapy. J. Cranio-Maxillofacial Surg. 45, 364–370. https://doi.org/10.1016/j.jcms.2017.01.005.

Chaukura, N., Katengeza, G., Gwenzi, W., Mbiriri, C.I., Nkambule, T.T., Moyo, M., Kuvarega, A.T., 2020. Development and evaluation of a low-cost ceramic filter for the removal of methyl orange, hexavalent chromium, and Escherichia coli from water. Mater. Chem. Phys. 249, 122965 https://doi.org/10.1016/j.matchemphys.2020.122965.

Chung, Y.-C., Chen, C.-Y., 2008. Antibacterial characteristics and activity of acid-soluble chitosan. Bioresour. Technol. 99, 2806–2814. https://doi.org/10.1016/j.biortech.2007.06.044.

de Oliveira, E.F., Yang, X., Basnayake, N., Huu, C.N., Wang, L., Tikekar, R., Nitin, N., 2021. Screening of antimicrobial synergism between phenolic acids derivatives and UV-A light radiation. J. Photochem. Photobiol. B Biol. 214, 112081 https://doi.org/10.1016/j.jphotobiol.2020.112081.

Deák, Á., Janovák, L., Tallósy, S.P., Bitó, T., Sebők, D., Buzás, N., Pálinkó, I., Dékány, I., 2015. Spherical LDH–Ag°-Montmorillonite Heterocoagulated System with a pH-Dependent Sol–Gel Structure for Controlled Accessibility of AgNPs Immobilized on the Clay Lamellae. Langmuir 31, 2019–2027. https://doi.org/10.1021/la504096t.

Dutheil de la Rochère, A., Evstratov, A., Bayle, S., Sabourin, L., Frering, A., Lopez-Cuesta, J.-M., 2019. Exploring the antimicrobial properties of dark-operating ceramic-based nanocomposite materials for the disinfection of indoor air. PLoS One 14, e0224114. https://doi.org/10.1371/journal.pone.0224114.

Fei Liu, X., Lin Guan, Y., Zhi Yang, D., Li, Z., De Yao, K., 2001. Antibacterial action of chitosan and carboxymethylated chitosan. J. Appl. Polym. Sci. 79, 1324–1335. https://doi.org/10.1002/1097-4628(20010214)79:7<1324::AID-APP210>3.0.CO;2-L.

Ferreira, O., Rijo, P., Gomes, J., Santos, R., Monteiro, S., Guedes, R., Serralheiro, M.L., Gomes, M., Gomes, L.C., Mergulhão, F.J., Silva, E.R., 2021. Antimicrobial Ceramic Filters for Water Bio-Decontamination. Coatings 11, 323. https://doi.org/10.3390/coatings11030323.

Gautam, L., Jain, J.K., Kalla, P., Choudhary, S., 2021. A review on the utilization of ceramic waste in sustainable construction products. Mater. Today Proc. 43, 1884–1891. https://doi.org/10.1016/j.matpr.2020.10.829.

Goodman, B.A., 2020. Utilization of waste straw and husks from rice production: a review. J. Bioresour. Bioprod. 5, 143–162. https://doi.org/10.1016/j.jobab.2020.07.001.

Hall, D.G., 2019. Boronic acid catalysis. Chem. Soc. Rev. 48, 3475–3496. https://doi.org/10.1039/C9CS00191C.

Harech, M.A., Mesnaoui, M., Abouliatim, Y., El Hafiane, Y., Benhammou, A., Abourriche, A., Smith, A., Nibou, L., 2021. Effect of temperature and clay addition on the thermal behavior of phosphate sludge. Boletín la Soc. Española Cerámica y Vidr. 60, 194–204. https://doi.org/10.1016/j.bsecv.2020.03.002.

Hossain, S.S., Roy, P.K., 2020. Sustainable ceramics derived from solid wastes: a review. J. Asian Ceram. Soc. 8, 984–1009. https://doi.org/10.1080/21870764.2020.1815348.

Kamaruzzaman, N.F., Tan, L.P., Hamdan, R.H., Choong, S.S., Wong, W.K., Gibson, A.J., Chivu, A., Pina, M., 2019. Antimicrobial Polymers: the potential Replacement of existing Antibiotics? Int. J. Mol. Sci. 20, 2747. https://doi.org/10.3390/ijms20112747.

Kim, S., Chung, J., Lee, S.H., Yoon, J.H., Kweon, D.-H., Chung, W.-J., 2021. Tannic acid-functionalized HEPA filter materials for influenza virus capture. Sci. Rep. 11, 979. https://doi.org/10.1038/s41598-020-78929-4.

Li, F., Kang, Z., Huang, X., Wang, X.-G., Zhang, G.-J., 2014. Preparation of zirconium carbide foam by direct foaming method. J. Eur. Ceram. Soc. 34, 3513–3520. https://doi.org/10.1016/j.jeurceramsoc.2014.05.029.

Liu, X., Ma, B., Tan, H., Jian, S., Lv, Z., Chen, P., Zhang, T., Qi, H., Wang, P., Lu, W., 2021. Utilization of turmeric residue for the preparation of ceramic foam. J. Clean. Prod. 278, 123825 https://doi.org/10.1016/j.jclepro.2020.123825.

Mouiya, M., Abourriche, A., Benhammou, A., El Hafiane, Y., Abouliatim, Y., Nibou, L., Oumam, M., Hannache, H., Smith, A., 2017. Porous ceramic from Moroccan natural phosphate and raw clay for microfiltration applications. Desalin. Water Treat. 83, 277–280. https://doi.org/10.5004/dwt.2017.20832.

Mouiya, M., Abourriche, A., Bouazizi, A., Benhammou, A., El Hafiane, Y., Abouliatim, Y., Nibou, L., Oumam, M., Ouammou, M., Smith, A., Hannache, H., 2018. Flat ceramic microfiltration membrane based on natural clay and Moroccan phosphate for desalination and industrial wastewater treatment. Desalination 427, 42–50. https://doi.org/10.1016/j.desal.2017.11.005.

Mullet, M., 1997. Surface electrochemical properties of mixed oxide ceramic membranes: Zeta-potential and surface charge density. J. Memb. Sci. 123, 255–265. https://doi.org/10.1016/S0376-7388(96)00220-7.

Nakamura, S., Kobayashi, T., Yamashita, K., 2002. Extended bioactivity in the proximity of hydroxyapatite ceramic surfaces induced by polarization charges. J. Biomed. Mater. Res. 61, 593–599. https://doi.org/10.1002/jbm.10224.

Napoli, C., Marcotrigiano, V., Montagna, M.T., 2012. Air sampling procedures to evaluate microbial contamination: a comparison between active and passive methods in operating theatres. BMC Public Health 12 (1), 594. https://doi.org/10.1186/1471-2458-12-594.

Noralian, Z., Gashti, M.P., Moghaddam, M.R., Tayyeb, H., Erfanian, I., 2021. Ultrasonically developed silver/iota-carrageenan/cotton bionanocomposite as an efficient material for biomedical applications. Int. J. Biol. Macromol. 180, 439–457. https://doi.org/10.1016/j.ijbiomac.2021.02.204.

Nunes, M.A.P., Gois, P.M.P., Rosa, M.E., Martins, S., Fernandes, P.C.B., Ribeiro, M.H.L., 2016. Boronic acids as efficient cross linkers for PVA: synthesis and application of tunable hollow microspheres in biocatalysis. Tetrahedron 72, 7293–7305. https://doi.org/10.1016/j.tet.2016.02.017.

Parvinzadeh Gashti, M., Dehghan, N., 2020. Gel diffusion-inspired biomimetic calcium iodate/gelatin composite particles: Structural characterization and antibacterial activity. J. Solid State Chem. 285, 121262 https://doi.org/10.1016/j.jssc.2020.121262.

Peng, H.X., Fan, Z., Evans, J.R.G., 2000. Factors affecting the microstructure of a fine ceramic foam. Ceram. Int. 26, 887–895. https://doi.org/10.1016/S0272-8842(00)00032-8.

Qiu, H., Si, Z., Luo, Y., Feng, P., Wu, X., Hou, W., Zhu, Y., Chan-Park, M.B., Xu, L., Huang, D., 2020. The Mechanisms and the applications of Antibacterial Polymers in Surface Modification on Medical Devices. Front. Bioeng. Biotechnol. 8 https://doi.org/10.3389/fbioe.2020.00910.

Reis, B., Gerlach, N., Steinbach, C., Haro Carrasco, K., Oelmann, M., Schwarz, S., Müller, M., Schwarz, D., 2021. A Complementary and revised View on the N-Acylation of Chitosan with Hexanoyl Chloride. Mar. Drugs 19, 385. https://doi.org/10.3390/md19070385.

Sirviö, J.A., Kantola, A.M., Komulainen, S., Filonenko, S., 2021. Aqueous Modification of Chitosan with Itaconic Acid to produce strong Oxygen Barrier Film. Biomacromolecules 22, 2119–2128. https://doi.org/10.1021/acs.biomac.1c00216.

Socrates, G., 2001. Infrared and Raman Characteristic Group Frequencies: Tables and Charts, third ed. J. Wiley and Sons, Chichester.

Stipniece, L., Kondratjeva, A., Salma-Ancane, K., 2020. Influence of precursor characteristics on properties of porous calcium phosphate-titanium dioxide composite bioceramics. Ceram. Int. 46, 243–250. https://doi.org/10.1016/j.ceramint.2019.08.257.

Tallósy, S.P., Janovák, L., Nagy, E., Deák, Á., Juhász, Á., Csapó, E., Buzás, N., Dékány, I., 2016. Adhesion and inactivation of Gram-negative and Gram-positive bacteria on photoreactive TiO2/polymer and Ag–TiO2/polymer nanohybrid films. Appl. Surf. Sci. 371, 139–150. https://doi.org/10.1016/j.apsusc.2016.02.202.

Tawema, P., Han, J., Vu, K.D., Salmieri, S., Lacroix, M., 2016. Antimicrobial effects of combined UV-C or gamma radiation with natural antimicrobial formulations against Listeria monocytogenes, Escherichia coli O157: H7, and total yeasts/molds in fresh cut cauliflower. LWT - Food Sci. Technol. 65, 451–456. https://doi.org/10.1016/j.lwt.2015.08.016.

Wang, F., Si, Y., Yu, J., Ding, B., 2021. Tailoring Nanonets-Engineered Superflexible Nanofibrous Aerogels with Hierarchical Cage-like Architecture Enables Renewable Antimicrobial Air Filtration. Adv. Funct. Mater. 31, 2107223. https://doi.org/10.1002/adfm.202107223.

Wen, P., Wang, C., Song, L., Niu, L., Chen, H., 2021. Durability and Sustainability of Cement-Stabilized Materials based on utilization of Waste Materials: a Literature Review. Sustainability 13, 11610. https://doi.org/10.3390/su132111610.

Zhang, G., Seright, R.S., 2013. Effect of Concentration on HPAM Retention in Porous Media, in: Day 1 Mon, September 30, 2013. SPE. https://doi.org/10.2118/166265-MS.